Since January 2020 Elsevier has created a COVID-19 resource centre with free information in English and Mandarin on the novel coronavirus COVID-19. The COVID-19 resource centre is hosted on Elsevier Connect, the company's public news and information website.

Elsevier hereby grants permission to make all its COVID-19-related research that is available on the COVID-19 resource centre - including this research content - immediately available in PubMed Central and other publicly funded repositories, such as the WHO COVID database with rights for unrestricted research re-use and analyses in any form or by any means with acknowledgement of the original source. These permissions are granted for free by Elsevier for as long as the COVID-19 resource centre remains active.

Veterinary Microbiology 171 (2014) 74–86

Contents lists available at ScienceDirect

Veterinary Microbiology

journal homepage: www.elsevier.com/locate/vetmic

Effects of virulent and attenuated transmissible gastroenteritis virus on the ability of porcine dendritic cells to sample and present antigen

Shanshan Zhao, Qi Gao, Tao Qin, Yinyan Yin, Jian Lin, Qinghua Yu, Qian Yang *

Key Lab of Animal Physiology and Biochemistry, Ministry of Agriculture, College of Veterinary Medicine,. Nanjing Agricultural University, Weigang 1, Nanjing 210095, Jiangsu, PR China

ARTICLE INFO

Article history:
Received 18 December 2013
Received in revised form 10 March 2014
Accepted 12 March 2014

Keywords:
Virulent and attenuated transmissible gastroenteritis virus (TGEV)
Monocyte-derived dendritic cells (Mo-DCs)
Intestinal DCs
Major histocompatibility complex classes II (SLA-II-DR)
T-cell proliferation

ABSTRACT

Virulent transmissible gastroenteritis virus (TGEV) results in an acute, severe pathology and high mortality in piglets, while attenuated TGEV only causes moderate clinical reactions. Dendritic cells (DCs), through uptake and presentation of antigens to T cells, initiate distinct immune responses to different infections. In this study, an attenuated TGEV (STC3) and a virulent TGEV (SHXB) were used to determine whether porcine DCs play an important role in pathogenetic differences between these two TGEVs. Our results showed that immature and mature monocyte-derived dendritic cells (Mo-DCs) were susceptible to infection with SHXB and STC3. However, only SHXB inhibited Mo-DCs to activate T-cell proliferation by down-regulating the expression of cell–surface markers and the secretion of cytokines *in vitro*. In addition, after 48 h of SHXB infection, there was the impairment in the ability of porcine intestinal DCs to sample the antigen, to migrate from the villi to the lamina propria and to activate T-cell proliferation *in vivo*. In contrast, these abilities of intestinal DCs were enhanced in STC3-infected piglets. In conclusion, our results show that SHXB significantly impaired the functions of Mo-DCs and intestinal DCs *in vitro* and *in vivo*, while STC3 had the opposite effect. These differences may underlie the pathogenesis of virulent and attenuated TGEV in piglets, and could help us to develop a better strategy to prevent virulent TGEV infection.

© 2014 Elsevier B.V. All rights reserved.

1. Introduction

Transmissible gastroenteritis virus (TGEV) belongs to the genus *coronavirus* of the family *Coronaviridae* (Masters, 2006). Virulent TGEV infection leads to severe vomiting, acute villous atrophy, malabsorptive diarrhoea and dehydration, which approach 100% mortality in seronegative suckling pigs. Even older piglets that recovered from virulent TGEV infections had impaired immune function (Woods, 2001). However, the piglets exposed to attenuated TGEV only had mild clinical signs and low mortality (Frederick et al., 1976). We presume that the interaction of TGEV with the immune cells has an important role in this pathogenesis.

Dendritic cells (DCs), the most powerful antigen-presenting cells (Ardavin, 2003), are widely distributed in the mucosal tissue, which forms an extensive network monitoring the invasion of pathogens (Haverson et al., 2000). Studies have demonstrated that viruses were directly or indirectly sampled by intestinal DCs (Rescigno et al., 2001). Thus, DCs are proposed to be among the first cells encountered after mucosal exposure to viruses. TGEV mainly infects and replicates in the porcine intestinal

* Corresponding author. Tel.: +86 02584395817; fax: +86 02584398669.
E-mail address: zxbyq@njau.edu.cn (Q. Yang).

http://dx.doi.org/10.1016/j.vetmic.2014.03.017
0378-1135/© 2014 Elsevier B.V. All rights reserved.

epithelial cells and must interact with the intestinal DCs. Recent studies have been suggested that the interaction between DCs and the different virulence of viruses plays an important role in the induction or inhibition of the immune response. Highly pathogenic avian influenza (HPAI) infection of chicken DCs could produce a lower level of cytokine in contrast to low pathogenic avian influenza (LPAI) infection (Vervelde et al., 2012). Lassa virus infection of human DCs could inhibit the upregulation of surface marker expression and the development of an adaptive immune response, while the related naturally non-virulent arenavirus Mopeia virus (MV) infection of DCs could increase the transcription of type I IFN mRNA, IL-12 mRNA and CXCL-10 mRNA and induce stronger T-cell responses (Baize et al., 2004; Pannetier et al., 2011). Similarly, virulent varicella-zoster virus (VZV) subverted secretion of Th1 cytokines in human DCs by blocking TLR2-mediated innate signals, while the attenuated VZV vaccine strain enhanced secretion of Th1 cytokines (Gutzeit et al., 2010). Thus, different responses of DCs to the virulent and attenuated virus may underlie the differences in pathogenicity between them.

Whether the varied morbidity and mortality in piglets caused by the differing virulence of TGEV infections is associated with the intestinal DCs is still unclear. In this study, the virulent TGEV (SHXB) and attenuated TGEV (STC3) strains were first used to infect porcine monocyte-derived dendritic cells (Mo-DCs) *in vitro* and evaluate the abilities of Mo-DCs to take up and present the antigens of the different virulent strains of TGEV, and stimulate the T-cell responses. Second, the SHXB and STC3 strains were used to infect the piglets *in vivo* in order to further determine whether they could damage the ability of intestinal DCs to sample the heat-inactivated *Escherichia coli*, migrate, and stimulate $CD3^+$, $CD4^+$ and $CD8^+$ T-cell proliferation at 48 h postinfection. Understanding these events may provide a theoretical basis for the study of the differences in pathogenesis of virulent and attenuated TGEV infection in pigs.

2. Materials and methods

2.1. Animals

A total of 46 six-week-old, Yorkshire, Landrace, and Large White cross-bred pigs were bred and maintained in a unique high sanitary state characterised by freedom from a wide range of porcine pathogens, *e.g.*, TGEV, PEDV, PCV-2, PRRSV. All animal experiments were carried out in accordance with the regulations and guidelines of laboratory animals of Nanjing Agriculture University (Nanjing, China).

2.2. Propagation of virus and E. coli k88

Two TGEV strains [SHXB, wild-virulent strain, verified by the animal attack virus test (see the Supplementary data (additional files 1–3)) and the STC3 live-attenuated strain (He et al., 2001)] were provided by the Jiangsu Academy of Agricultural Sciences (JAAS). The strains were propagated in Swine Testicle (ST) cells and were purified using a sucrose gradient as described previously (Krempl and Herrler, 2001). The viral 50% cell tissue infectious dose ($TCID_{50}$) of the purified SHXB and STC3 strains were calculated using the Reed and Muench method (Haggett and Gunawardena, 1964). *E. coli* K88 (enterotoxigenic *E. coli* k88, Invitrogen, USA) was grown overnight in Luria broth (LB). When the *E. coli* were at a concentration of 1–10^8 cfu ml^{-1}, they were heat killed in a water bath at 95 °C for 15 min. They were then diluted to the appropriate concentration in FCS-free cell culture medium for testing that there was no live *E. coli*.

2.3. Generation of Mo-DCs

Porcine Mo-DCs were generated as previously reported (Carrasco et al., 2001). Briefly, porcine peripheral blood mononuclear cells (PBMC) were separated from the blood of six piglets by density centrifugation using Histopaque (1.077 g l^{-1}) (Sigma, USA). PBMCs were washed three times in RPMI 1640 medium (Gibco, USA), and resuspended in complete RPMI 1640 medium with 10% FBS (MULTICell, Canada). PBMC were then placed in six-well plates and incubated overnight at 37 °C in 5% CO_2. The non-adherent cells were removed leaving the adherent monocytes. The monocytes were cultured in complete RPMI 1640 medium containing 20 ng ml^{-1} of pIL-4 (BioSource, USA) and 20 ng ml^{-1} of pGM-CSF (Invitrogen, USA) at 37 °C in 5% CO_2. Cells were incubated for five days to allow for their differentiation into immature Mo-DCs and replaced with cytokine-containing medium on day 3. Immature Mo-DCs were harvested on day 5 and resuspended in RPMI 1640 medium. For further induction of maturation, immature Mo-DCs were stimulated by the addition of 2 ug ml^{-1} of lipopolysaccharide (*Escherichia coli* O26:B6, Sigma, USA) for 24 h.

2.4. TGEV infection of Mo-DCs

Immature and mature Mo-DCs were inoculated with TGEV (SHXB or STC3) at a concentration of 100 $TCID_{50}$ $cell^{-1}$. The viruses were adsorbed for 1 h at 37 °C. In order to eliminate the non-absorbed virus, cells were washed five times with PBS, centrifuged at 200 × *g* for 5 min at 4 °C, and re-suspended in fresh RPMI 1640 medium containing pIL-4 and pGM-CSF. Mock-infected cells were treated in parallel. All Mo-DCs were seeded onto 6-well plates (5×10^5 cells/well) and cultured for the required incubation period.

2.5. Virus titration assay

SHXB- and STC3-infected immature and mature Mo-DCs were seeded onto 6-well plates (5×10^5) and cultured for 2, 9, 24, 48 h. The virus was collected by freezing and thawing the plates three times, and determined by the tissue culture infectious dose 50 ($TCID_{50}$) in ST cells.

2.6. Determination of SHXB- and STC3-infected Mo-DCs by flow cytometric analysis

SHXB- and STC3-infected immature and mature Mo-DCs were seeded onto 6-well plates (1×10^5) and cultured

for 12, 24, 48 h. The cell samples (1×10^5 cells) were washed with PBS twice and permeabilised for 5 min with 0.05% Triton X-100. The cells were incubated with a 1% solution of BSA for 30 min at room temperature and stained with FITC-conjugated TGEV polyclonal antibody (VMRD, USA) and PE-conjugated mouse anti-porcine monoclonal antibody to Swine Workshop Cluster 3a (SWC3a) (Abcam, Hongkong) for 30 min at 4 °C. Cells were then washed twice with 0.01 M PBS and then were resuspended in 200 μl of PBS. Samples of 1×10^4 cells were analysed by flow cytometry.

2.7. Determination of phenotype markers of Mo-DCs by flow cytometric analysis

To determine the modulation of the surface markers on Mo-DCs treated with TGEV after 24 h postinfection (p.i.), the cell samples (1×10^5 cells) were washed with PBS twice, and incubated for 30 min at 4 °C with appropriate dilutions of the following monoclonal antibodies: FITC-conjugated mouse anti-swine monoclonal antibody to swine histocompatibility leukocyte Ag II-DR (SLA-II-DR) (LifeSpan BioSciences, USA), FITC-conjugated mouse anti-human monoclonal antibody to the co-stimulatory molecules cluster of differentiation 80/86 (CD80/86) (Abcam, Hongkong), FITC-conjugated mouse anti-porcine monoclonal antibody to cluster of differentiation 1a (CD1a)(Abcam, Hongkong), and PE-conjugated mouse anti-porcine monoclonal antibody to Swine Workshop Cluster 3a (SWC3a)(Abcam, Hongkong). Cells washed twice with 0.01 M PBS and were resuspended in 200 μl of PBS. Samples of 1×10^4 cells were analysed by flow cytometry.

2.8. Apoptosis assay

The apoptosis of immature and mature Mo-DCs treated with the SHXB and STC3 strains was quantified at 24 h postinfection (p.i.). The dual parameter analysis of Annexin V-FITC (Invitrogen, USA) and propidium iodide (PI; Sigma, USA) was performed. Samples containing 5×10^5 Mo-DCs were labelled first with AnnexinV-FITC (2 mg ml^{-1}) for 15 min and then with PI (50 mg ml^{-1}). The samples were analysed by flow cytometry.

2.9. Enzyme-linked immunosorbent assay (ELISA)

ELISA was used to determine the concentration of IL-12, IFN-γ, and IL-10 in immature and mature Mo-DCs (1×10^6 cells/well) infected with SHXB and STC3 at 24 h p.i. The levels of the three cytokines were quantified in the supernatants using commercial ELISA kits (R&D Systems, USA), according to the manufacturer's recommendations.

2.10. Mixed leukocyte reaction (MLR) in porcine dendritic cells measured by flow cytometric analysis

MLR was evaluated by flow cytometry using the florescent dye carboxyfluorescein succinimidyl ester (CFSE; Sigma, MO, USA). To isolate T cells, the PBMCs were labelled with mouse anti-CD3 antibody (Abcam, Hongkong) followed by incubation with rat anti-mouse IgG1 microbeads (MACS; Miltenyi Biotec, Germany). Purified T lymphocytes (1×10^7) were stained with 0.1 μM CFSE in RPMI-1640 medium for 10 min at 37 °C and 5% CO_2 in the dark. TGEV-infected Mo-DCs were incubated simultaneously with mitomycin C (10 ug ml^{-1}) for 1 h. CFSE-labelled T-lymphocytes (5×10^5) were co-cultured with TGEV-infected DCs at a ratio of 1:1; 1:10; 1:100 (DCs: lymphocytes). Co-cultures were incubated at 37 °C in 5% CO_2 for five days. Finally, the cells were harvested, and the fluorescence intensity of the CFSE was determined by flow cytometric analysis.

2.11. Animal experimental design

The first animal experiment: A total of 20 conventional 1.5-month-old piglets were assigned to four groups, which were maintained in isolation facilities to prevent virus circulation. All piglets were starved 24 h before surgery to insure the least amount of chymus possible in the intestine. The treatments of these groups were showed in Table 1. In group I ($n1 = 5$), the piglets were anesthetised with pentobarbital sodium, and a midline incision was

Table 1
The first animal experiment design.

	Group and pig numbers	Inculation and numbers of segments per pig	Time of virus infection
Intestinal ligation	I ($n1 = 5$)	PBS (1 ml per segment, $n2 = 3$)	3 h (From the first injection to sacrifice)
		PBS (1 ml per segment, $n2 = 3$)	15 min (from the second injection to sacrifice)
		SHXB (1 ml of 1×10^7 $TCID_{50}$ ml^{-1} per segment, $n2 = 3$)	3 h (from the first injection to sacrifice)
			15 min (from the second injection to sacrifice)
		SHXB (1 ml of 1×10^7 $TCID_{50}$ ml^{-1} per segment, $n2 = 3$)	
	II ($n1 = 5$)	PBS (1 ml per segment, $n2 = 3$)	3 h (From the first injection to sacrifice)
		PBS (1 ml per segment, $n2 = 3$)	15 min (from the second injection to sacrifice)
		STC3 (1 ml of 1×10^7 $TCID_{50}$ ml^{-1} per segment, $n2 = 3$)	3 h (from the first injection to sacrifice)
			15 min (from the second injection to sacrifice)
		STC3 (1 ml of 1×10^7 $TCID_{50}$ ml^{-1} per segment, $n2 = 3$)	
Oral administ-ration	III ($n1 = 5$)	SHXB (20 ml of 1×10^7 $TCID_{50}$ ml^{-1} per pig)	48 h (From administration to sacrifice)
	IV ($n1 = 5$)	STC3 (20 ml of 1×10^7 $TCID_{50}$ ml^{-1} per pig)	48 h (from administration to sacrifice)

made just anterior to the navel (Nielsen and Sautter, 1968). Twelve jejunum segments containing the Peyer's patches (PPs) per piglet were divided into four treatments. The first treatment was injected with SHXB strain 3 h before sacrifice ($n2 = 3$), the second treatment was injected with sterile 0.0.1 M PBS 3 h before sacrifice ($n2 = 3$), the third was injected with SHXB strain 15 min before sacrifice ($n2 = 3$), the fourth was injected with sterile 0.0.1 M PBS 15 min before sacrifice ($n2 = 3$). During the procedure, pigs were kept warm on a 37 °C warming pad. The pigs were sacrificed and the twelve intestinal segments were removed. In group II ($n1 = 5$), except for STC3 strain, the surgery and the sample grouping were the same as groupI. Piglets in group III ($n1 = 5$) and group IV ($n1 = 5$) did not carry out the surgery, were separately inoculated with the SHXB strain and STC3 strain by oral administration. 48 h after the inoculation, the piglets were sacrificed and the three intestinal segments ($n2 = 3$) were collected. Upon washing with ice-chilled PBS, tissues were immediately fixed in 4% polyoxymethylene for histological processing. Half of the fixed tissues were embedded in OCT (a tissue-freezing medium, China), and then stored at −80 °C until further use. Frozen tissue sections (10-μm thick) were cut on a Leica CM 3050S cryostat and transferred to poly-L-lysine coated microscope slides. The slides were air-dried and stored for up to 6 weeks at −20 °C before immunofluorescence staining. Another half of the fixed tissues were embedded in paraffin wax using standard techniques. Slices (5-μm thick) were cut and stored for immunohistochemical staining.

The second animal experiment: In brief, a total of 20 conventional 1.5-month-old piglets were divided into four groups and the treatments of these groups were showed in Table 2. Piglets in group I ($n1 = 5$), group II ($n1 = 5$), group III ($n1 = 5$) and group IV ($n1 = 5$) were, respectively, inoculated with sterile PBS, sterile PBS, SHXB and STC3 by oral administration. At 48 h after infection, all piglets were subjected to the intestinal ligation as described above. In group I, 1 ml of PBS was injected into the intestinal segments ($n2 = 5$) 3 h and 15 min before sacrifice as negative controls. In groups II–IV, the heat-inactivated *E. coli* were injected into the intestinal segments ($n2 = 5$) 3 h and 15 min before sacrifice. Piglets were then sacrificed and the segments were removed. The following treatments were the same as described above.

2.12. Immunofluorescence staining

Three-colour fluorescent immunohistology was carried out on cryosections. Fc receptors were blocked for 30 min with phosphate-buffered saline (PBS) containing 5% pig serum. Combinations of FITC-SLA-DR$^+$PE-SWC3a$^+$ or CD16$^+$CD11b$^+$ (Abcam, Hongkong) primary mAbs were added to the slides overnight at 4 °C. Subsequently, AlexaFluor 594-conjugated donkey anti-goat IgG2b and AlexaFluor 488-conjugated donkey anti-mouse IgG1 (Invitrogen, USA) were added for 1 h at room temperature. Cell nuclei were stained by a 2-min incubation with 4,6-diamidino-2-phenylindole (DAPI) solution (Invitrogen, USA). Each incubation step was followed by washing steps (2×5 min each) in fresh changes of TBS-Tween. Labelled sections were sealed with nail varnish and stored at 4 °C. The negative control slides were treated in an identical manner except the primary antibodies were omitted.

2.13. Immunohistochemistry

In brief, paraffin sections were dewaxed in xylene and rehydrated in decreasing concentrations of ethanol. Slides were blocked with serum as described above for immunofluorescence staining. Subsequently, porcine CD3$^+$, CD4$^+$, CD8$^+$ T cells primary antibody (Abcam, Hong Kong) were, respectively, applied to the sections overnight at 4 °C. Subsequently, the slides were incubated for another 1 h with an ABC-based system (biotinylated goat anti-mouse antibody was used as the secondary antibody with DAB as a chromogen). Finally, the slides were counter-stained with hematoxylin and mounted for examination. The negative control slides were treated in an identical manner except the primary antibodies were omitted.

2.14. Microscopic analysis

Slides were examined on an Axioplan 2 microscope (Carl Zeiss, Oberkochen, Germany) or on a Leica DMRE7 fluorescence microscope (Leica, Bensheim, Germany). Digital images were recorded on a Spot RT digital camera by using Spot Advanced software (Diagnostic Instruments, Sterling Heights, MI, USA). Measurements and cell counts

Table 2
The second animal experiment design.

Group and pig numbers	Oral administration and time of infection	Inculation and numbers of segments per pig	Time of HI-*E. coli* inoculation
I ($n1 = 5$)	PBS (20 ml, 48 h)	PBS (1 ml per segment, $n2 = 3$)	3 h (From the first injection to sacrifice)
		PBS (1 ml per segment, $n2 = 3$)	15 min (From the second injection to sacrifice)
II ($n1 = 5$)	PBS (20 ml, 48 h)	HI-*E. coli* (1 ml of 1×10^8 cfu ml^{-1} per segment, $n2 = 3$)	3 h (From the first injection to sacrifice)
		HI-*E. coli* (1 ml of 1×10^8 cfu ml^{-1} per segment, $n2 = 3$)	15 min (From the second injection to sacrifice)
III ($n1 = 5$)	SHXB (20 ml of 1×10^7 $TCID_{50}$ ml^{-1}	HI-*E. coli* (1 ml of 1×10^8 cfu ml^{-1} per segment, $n2 = 3$)	3 h (From the first injection to sacrifice)
	per pig, 48 h)	HI-*E. coli* (1 ml of 1×10^8 cfu ml^{-1} per segment, $n2 = 3$)	15 min (From the second injection to sacrifice)
IV ($n1 = 5$)	STC3 (20 ml of 1×10^7 $TCID_{50}$ ml^{-1} per pig, 48 h)	HI-*E. coli*(1 ml of 1×10^8 cfu ml^{-1} per segment, $n2 = 3$)	3 h (From the first injection to sacrifice)
		HI-*E. coli*(1 ml of 1×10^8 cfu ml^{-1} per segment, $n2 = 3$)	15 min (From the second injection to sacrifice)

were performed by using ImagePro 6.0 (Media Cybernetics, Silver Spring, MD, USA). DC positive results were measured by the mean number of the positive cells per mm^2 of tissue section, and T cell positive results were expressed as the integral optical density (IOD).

2.15. Statistical analysis

The statistical analysis was performed using the Statistical Product and Services Solutions (SPSS) package, version 16.0. Duncan's test was conducted to determine the differences among treated groups. The means of paired groups were analysed by ANOVA. Significance was indicated by a probability of $P < 0.05$.

3. Results

3.1. Morphology of Mo-DCs

In order to differentiate into Mo-DCs, porcine monocytes were cultured for five days using RPMI 1640 media with rpGM-CSF and rpIL-4. The immature Mo-DCs became semi-suspended or suspended, with a round appearance and dendritic processes, and often formed clusters at five days (Fig. 1A, left). Mo-DCs stimulated with LPS for 24 h assumed a typical DC-like morphology, including a significant size, irregular shape, presenting either as single cells or in clusters on the cell surface at six days (Fig. 1A, right).

3.2. Infection of Mo-DCs by SHXB and STC3

It is already known that TGEV could infect porcine alveolar macrophages (PAMs) (Laude et al., 1984). Our results showed that the viral titres of SHXB and STC3 strains in the immature and mature Mo-DCs both persistently increased over time, and the two viral titres in the immature Mo-DCs were higher than in the mature Mo-DCs (Fig. 1B), which demonstrated that immature Mo-DCs were more susceptible to the two strains. However, there was no significance between SHXB titre and STC3 titre in the immature and mature Mo-DCs. Next, the percentage of infected Mo-DCs at different times was detected by flow cytometry. The results showed that the

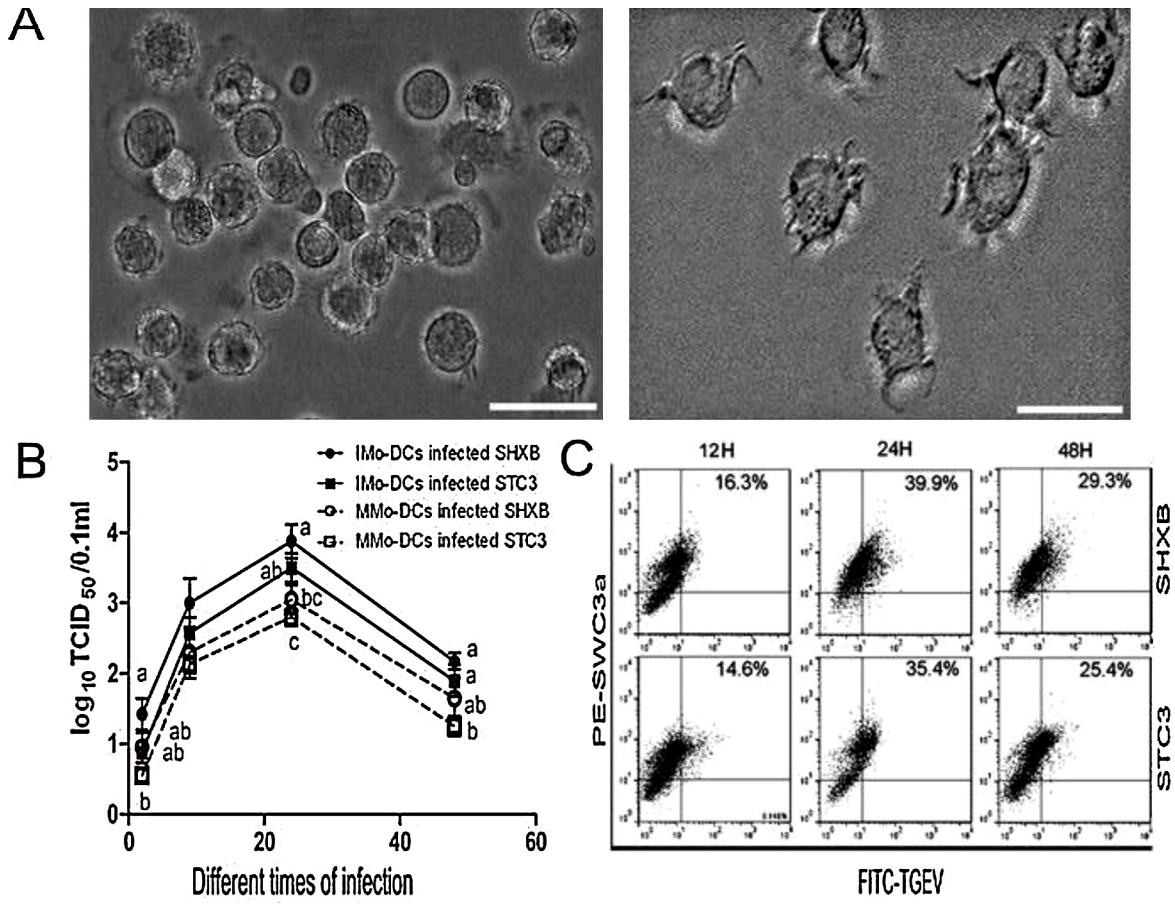

Fig. 1. *Morphology of Mo-DCs and infection of TGEV.*
(A) Images show the morphology of immature (left) and mature Mo-DCs (right) by optical microscopy. Scale bars represent 50 nm. (B) The viral titres of SHXB and STC3 in the immature and mature Mo-DCs at 2, 9, 24, and 48 h postinfection (p.i.). Data express the mean ± SEM ($n = 3$). Bars labelled with different letters are significantly different from each other ($P < 0.05$). (C) Dot plots show the percentage of infected immature Mo-DCs at 12, 24, and 48 h p.i. using FITC-labelled-TGEV-polyclonal antibody and flow cytometry.

percentage of infected immature and mature Mo-DCs reached a peak at 24 h. p.i., then gradually decreased at 48 h. p.i. (Fig. 1C).

3.3. Phenotypic alterations and apoptosis in SHXB- and STC3-infected Mo-DCs

To determine whether SHXB and STC3 infection could affect Mo-DC maturation, we analysed surface marker expression of CD1a, CD80/86 and SLA-II-DR on the Mo-DCs. When compared to the immature Mo-DCs, mature Mo-DCs stimulated by LPS significantly upregulated CD1a and SLA-II-DR expression (Fig. 2A and B). However, the expression of CD1a clearly decreased in the immature and mature Mo-DCs infected with SHXB compared with the others, and the expression of SLA-II-DR in the immature Mo-DCs infected with SHXB was also lower than others (Fig. 2A and B). The level of CD1a and SLA-II-DR in the immature and mature Mo-DCs infected with STC3 was similar with the control immature Mo-DCs (Fig. 2A and B). The results also showed that CD80/86 expression in the immature and mature Mo-DCs infected with SHXB and STC3 remained unchanged (Fig. 2A and B). The down-regulation of co-stimulatory molecules on immature and

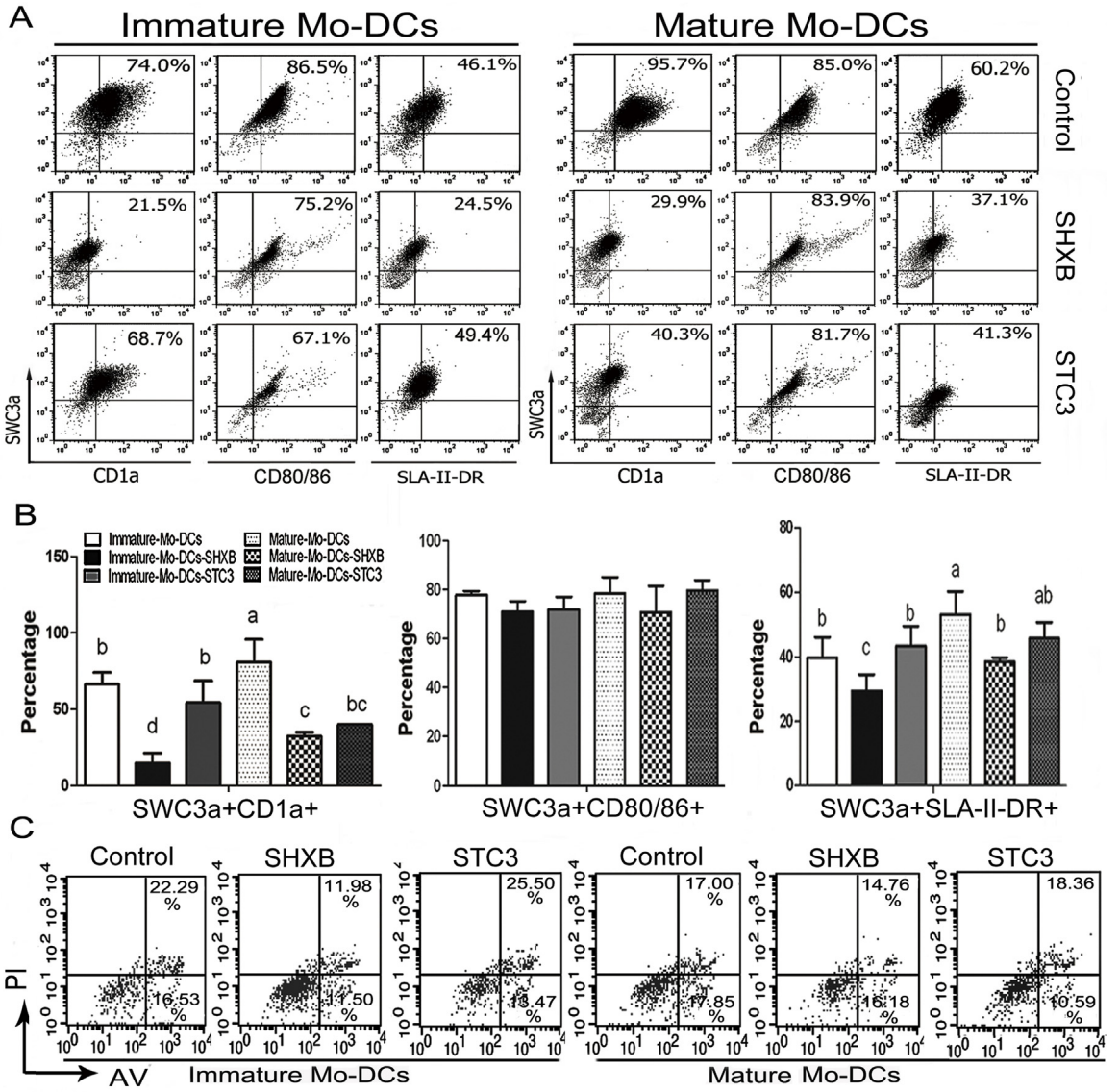

Fig. 2. *Expression of CD1a$^+$ SWC3a$^+$, CD80/86$^+$ SWC3a$^+$ and SLA-II-DR$^+$ SWC3a$^+$ by immature and mature Mo-DCs infected with SHXB and STC3 at 24 h p.i. and the apoptosis at 24 h p.i.*

(A) Dot plots show the percentage of CD1a$^+$SWC3a$^+$, CD80/86$^+$SWC3a$^+$ and SLA-II-DR$^+$SWC3a$^+$ Mo-DCs in the immature (left) and mature (right) Mo-DCs infected with SHXB and STC3 among the total Mo-DCs. (B) Bar graphs show the number of CD1a$^+$SWC3a$^+$, CD80/86$^+$SWC3a$^+$ and SLA-II-DR$^+$SWC3a$^+$ cells in the immature and mature Mo-DC populations infected with SHXB and STC3. Data express the mean ± SEM ($n = 3$). Bars labelled with different letters are significantly different from each other ($P < 0.05$). (C) Dot plots show the percentage of apoptotic immature and mature Mo-DCs treated with SHXB and STC3 at 24 h p.i.

mature Mo-DCs may be a mechanism for virus immune escape for impairing DCs maturation, which may render Ag-specific T cells anergy or suppress the T-cell response. Next, the SHXB and STC3 infection did not induce the early and late apoptosis of the immature and mature Mo-DCs (Fig. 2C), which indicated that the downregulation of surface makers on immature and mature Mo-DCs infected with SHXB was not related to the apoptosis induced by the SHXB.

3.4. Cytokine secretion of Mo-DCs treated with SHXB and STC3

DCs are able to orchestrate immune responses not only through the expression of surface molecules, but also by secreting cytokines. Our results showed that the mature Mo-DCs stimulated by LPS resulted in significant secretion of the three cytokines as compared with immature Mo-DCs (Fig. 3A). The levels of IL-12 and IFN-γ in virulent SHXB-infected immature Mo-DCs was higher than in controls, but notably lower than those in STC3- and LPS-stimulated immature Mo-DCs. However, the secretion of IL-12 and IFN-γ in SHXB- and STC3-infected mature Mo-DCs was not significant. The levels of IL-10 in both SHXB- and STC3-infected immature and mature Mo-DCs did not differ significantly from control immature Mo-DCs (Fig. 3A). The results showed that the virulent SHXB strain made immature and mature Mo-DCs produce the limit of IL-12, IFN-γ for clearance itself, while the attenuated STC3 could induce the immature Mo-DCs to secrete a considerable amount of IL-12 and IFN-γ for activation of an immune response. However, neither SHXB nor STC3 could stimulate the secretion of IL-10.

3.5. T cell proliferation stimulated by SHXB- and STC3-infected immature Mo-DCs

The Mixed Leukocyte Reaction was used to determine whether the ability of SHXB- and STC3-infected Mo-DCs to stimulate T-cell proliferation had been damaged *in vitro*. Our results showed that the mature Mo-DCs treated by LPS were more stimulatory than immature Mo-DCs at DC/T cell ratios of 1:1, 1:10 and 1:100 (Fig. 3B). SHXB-infected immature and mature Mo-DCs had almost no stimulatory capacity on T cell proliferation at DC/T cell ratios of 1:1, 1:10 and 1:100, while the STC3-infected immature and mature Mo-DCs had a stronger ability to activate T cells at a DC/T cell ratio of 1:1 (Fig. 3B).

3.6. SHXB and STC3 infection effects on the intestinal DCs in vivo

The SHXB and STC3 strains were administered to the piglets, and the intestinal DCs were visualised in serial cryosections at 15 min, 3 h and 48 h p.i. From Fig. 4A–C, the $CD11b^{+}CD16^{+}$ DCs and $SWC3a^{+}SLA\text{-}II\text{-}DR^{+}$ DCs rapidly increased in small intestine villi and lamina propria after 15 min of injecting SHXB, but gradually decreased from 3 to 48 h after SHXB infection. There was almost no change in the number of these DCs in the small intestinal villi and lamina propria after 15 min, but the number gradually increased from 3 to 48 h after STC3 infection. These results implied that $CD11b^{+}$ $CD16^{+}$ DCs and $SWC3a^{+}SLA\text{-}II\text{-}DR^{+}$ DCs had a strong ability to uptake and present the SHXB in early infection of piglets, then significantly decreased with time, while the capability of these DCs to take up and present STC3 gradually enhanced with time.

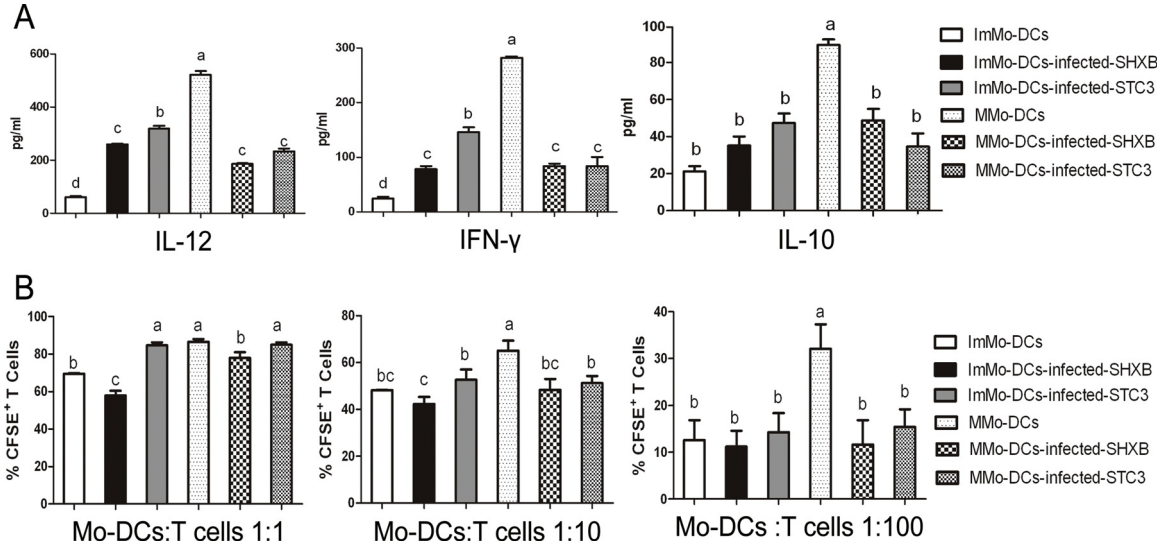

Fig. 3. *Cytokine production by immature and mature Mo-DCs treated with SHXB and STC3, and T cell activation stimulated by the virulent SHXB- and STC3-infected immature and mature Mo-DCs.*
(A) Bar graphs show the production of three cytokines in immature Mo-DCs infected with SHXB and STC3, including Interleukin-12 (left), Interferon-γ (middle) and Interleukin-10 (right). (B) SHXB- and STC3-infected immature and mature Mo-DCs (24 h p.i.) were co-cultured with T lymphocytes (ratios 1:1, 1:10 and 1:100). Five days after infection, co-culture proliferation was evaluated using CFSE. Data represent the mean ± SEM ($n = 3$). Bars showing different letters represent values significantly different from each other ($P < 0.05$).

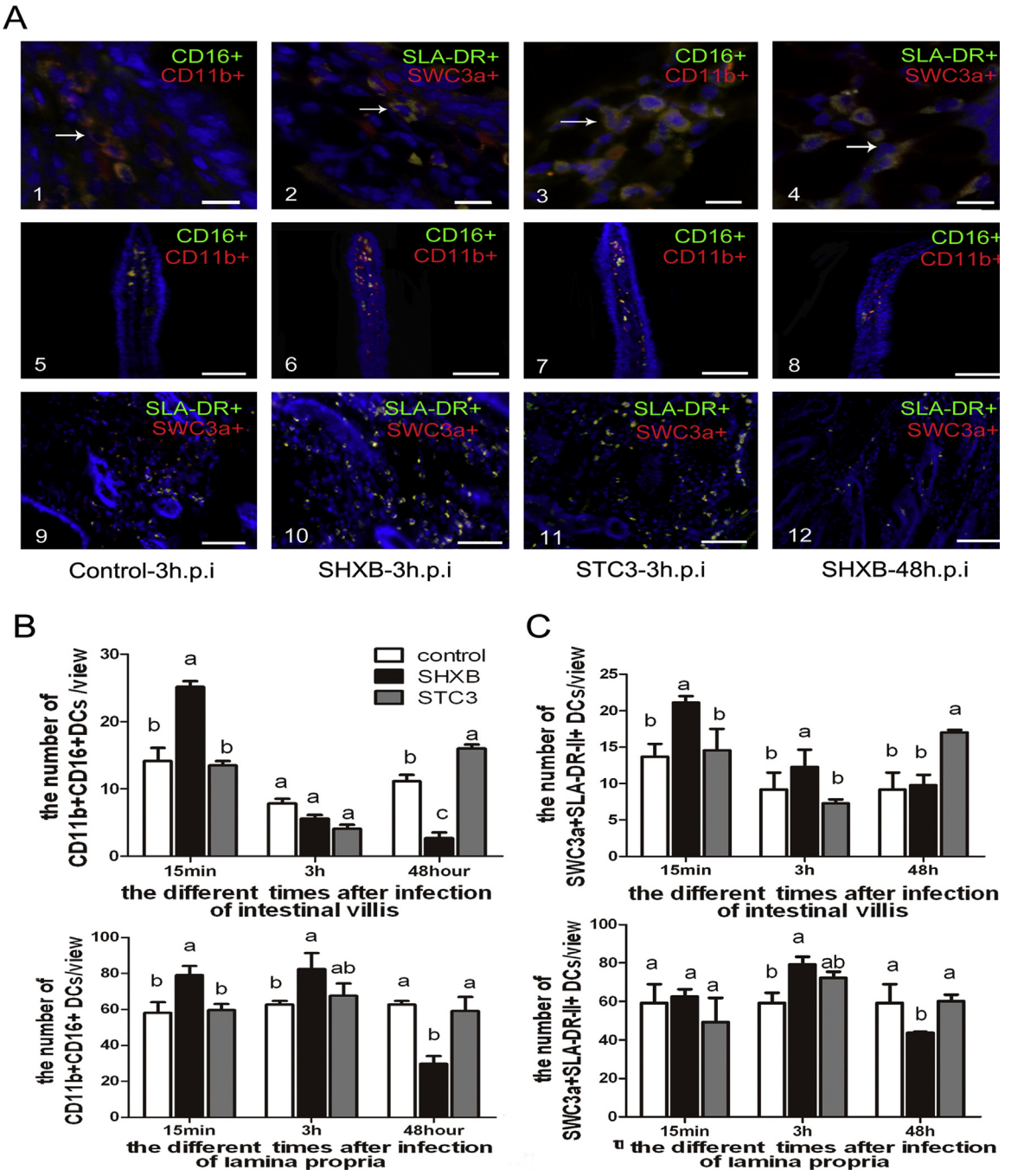

Fig. 4. *Effect on the number of CD11b$^+$ CD16$^+$ DCs and SWC3a$^+$ SLA-II-DR$^+$ DCs in the intestinal villi and lamina propria by SHXB- and STC3-infected piglets.* (A) Images 1 and 3 show the morphology the CD11b$^+$CD16$^+$ DCs in the intestinal villi and lamina propria. Images 2 and 4 show the morphology of SWC3a$^+$SLA-II-DR$^+$ DCs in intestinal villi and the lamina propria. Scale bars represent 10 nm. Images 5–8 and 9–12 show the number of changes in CD11b$^+$ CD16$^+$ DCs and SWC3a$^+$ SLA-II-DR$^+$ DCs in the intestinal villi of control piglets, SHXB- and STC3-infected piglets. Images are shown at 200× magnification. Scale bars represent 100 nm. Bar graphs show the number of CD11b$^+$CD16$^+$ DCs (B) and SWC3a$^+$ SLA-II-DR$^+$ DCs (C) of the intestinal villus and lamina propria in piglets after 15 min, 3 h and 48 h of infection with SHXB and STC3. Data express the mean ± SEM ($n = 5$). Bars labelled with different letters are significantly different from each other ($P < 0.05$).

3.7. SHXB and STC3 infection effects on intestinal T cell subsets in vivo

From the immunohistochemical staining pictures *in vivo* (Fig. 5A), the CD3$^+$, CD4$^+$ and CD8$^+$ T cells were mainly distributed in the lamina propria, and a small number were distributed in the intestinal villi when the piglets were infected with virulent and attenuated TGEV. At 15 min and 3 h after SHXB and STC3 infection, the IOD of the CD3$^+$, CD4$^+$ T cells in the porcine intestinal villi and lamina

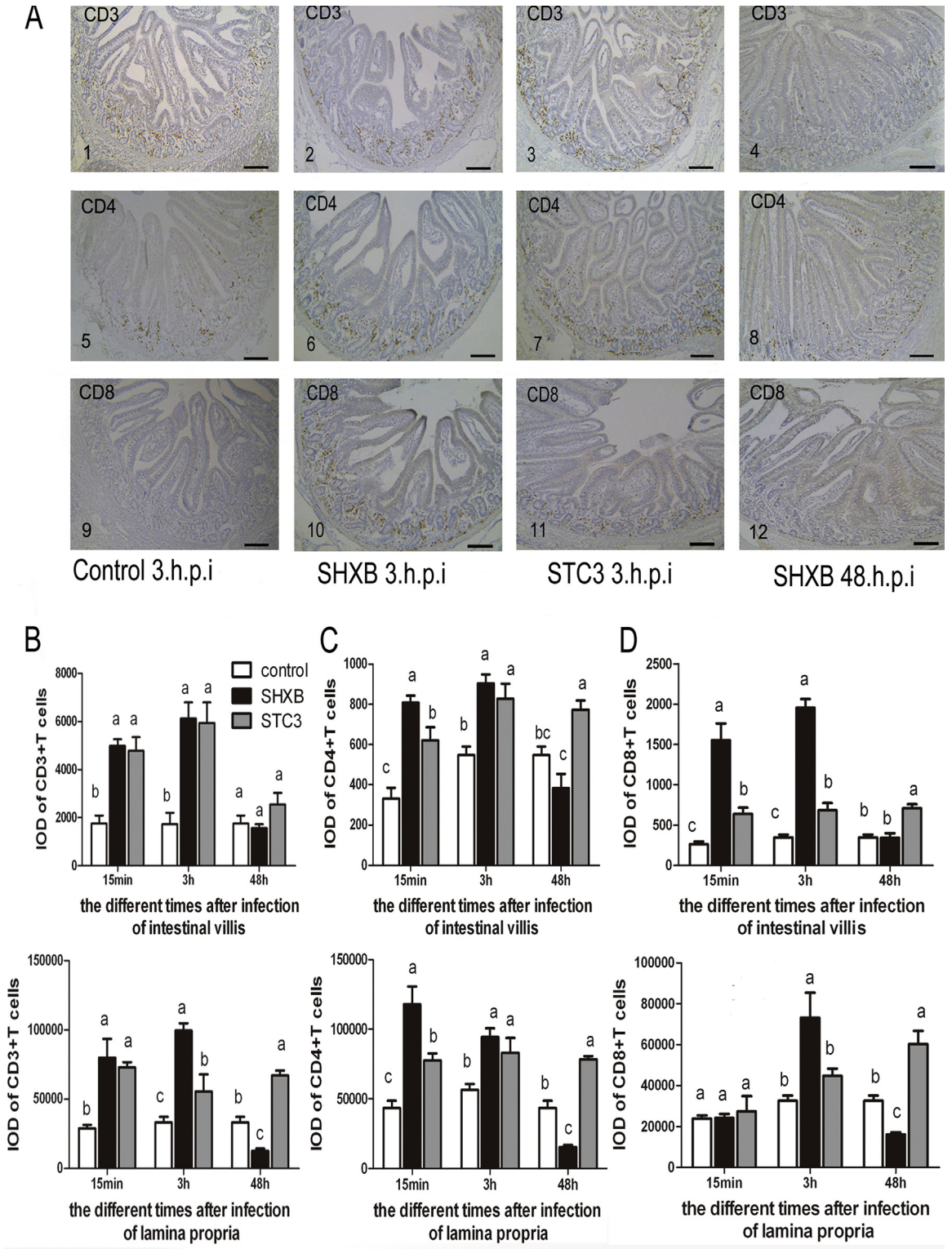

Fig. 5. *Effect on T lymphocyte proliferation by SHXB- and STC3-infected immature and mature Mo-DCs and intestinal DCs.*
(A) Images 1–4, 5–8 and 9–12 show the number changes of $CD3^+$, $CD4^+$, and $CD8^+$ T cells in the intestinal villi and lamina propria of control piglets, SHXB- and STC3-infected piglets. Scale bars represent 180 nm. (B) Bar graphs show the number of $CD3^+$ T cells in the intestinal villus and lamina propria, (C) the $CD4^+$ T cells in the intestinal villus and lamina propria, (D) and the $CD8^+$ T cells in the intestinal villus and lamina propria by SHXB- and STC3-infected piglets at 15 min, 3 h and 48 h postinfection. Data express the mean ± SEM ($n = 5$). Bars labelled with different letters are significantly different from each other ($P < 0.05$).

propria was significantly higher than in the control group, and the $CD8^+$ T cells in the intestinal villi of SHXB infected piglets was also significantly higher than in the control group (Fig. 5B–D). After 48 h of piglet infection with STC3, the $CD3^+$ T cells in the lamina propria and the $CD4^+$and $CD8^+$ T cells in the intestinal villi and lamina propria were still significantly higher than in the control group, whereas they significantly decreased after 48 h of infection with SHXB (Fig. 5B–D). These results indicated that the number of $CD3^+$, $CD4^+$ and $CD8^+$ T cells rapidly increased to cause a strong immune response when piglets were infected early with virulent and attenuated TGEV. After 48 h of infection, T-cell proliferation was inhibited because of the damaged function of intestinal DCs in the SHXB-infected piglets. However, T-cell proliferation was significantly enhanced due to the improved function of intestinal DCs in the STC3-infected piglets.

3.8. Virulent TGEV infection damaged the functions of porcine intestinal DCs and T cell subsets

The SHXB strain could damage the functions of intestinal DCs, and the STC3 strain could enhance these

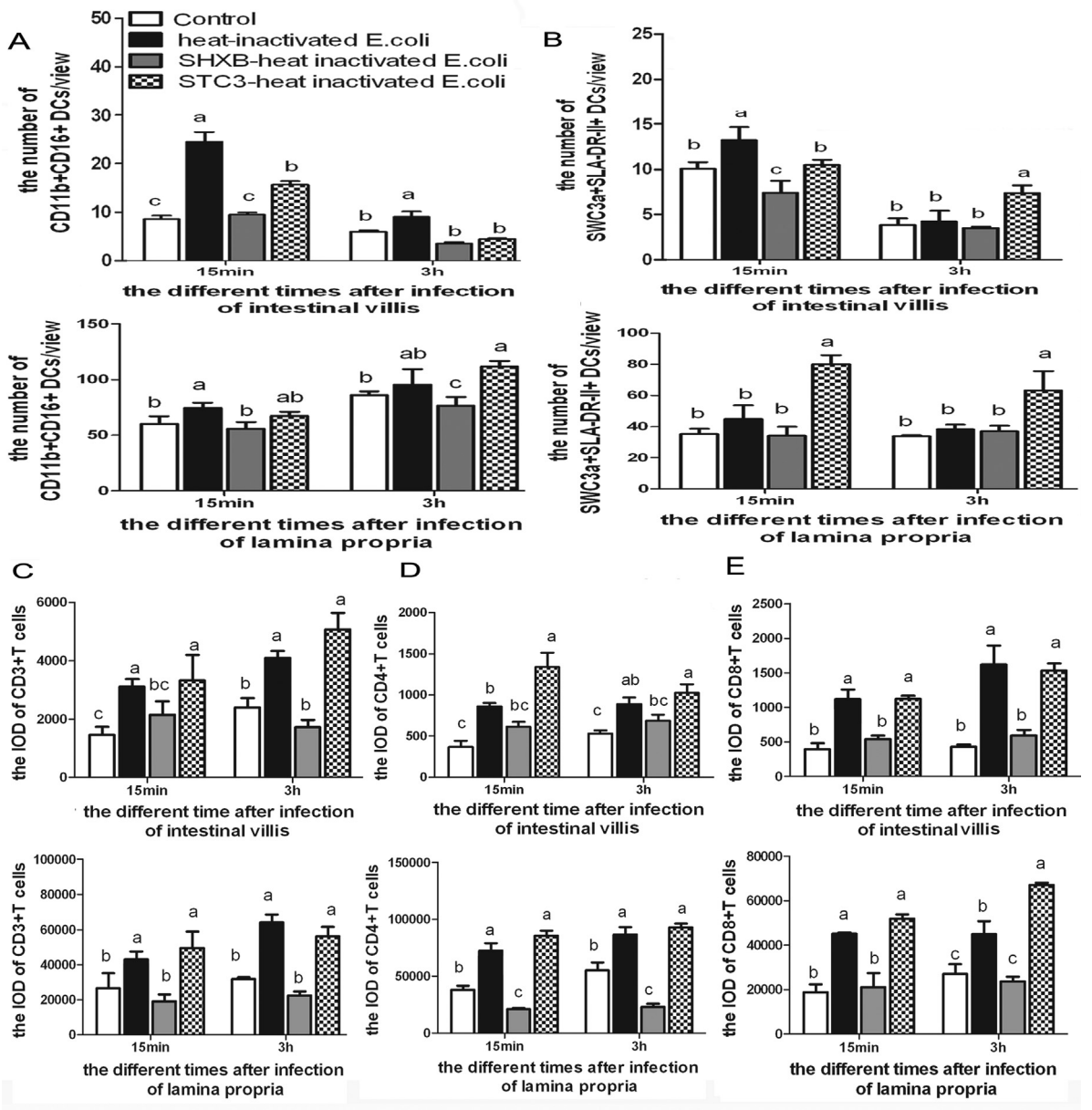

Fig. 6. *Effect on the ability of intestinal $CD11b^+$ $CD16^+$ DCs and $SWC3a^+$ SLA-II-DR^+ DCs to sample the heat-inactivated E. coli, migrate and stimulate T cell proliferation in SHXB- and STC3-infected piglets.*

Bar graphs show the number of $CD11b^+CD16^+$ DCs (A) and $SWC3a^+$SLA-II-DR^+ DCs (B) in the intestinal villus and lamina propria that sampled the heat-inactivated *E. coli* and migrated at 48 h postinfection with SHXB and STC3. Bar graphs show the proliferation of $CD3^+$ (C), $CD4^+$ (D), and $CD8^+$ (E) T cells in the intestinal villus and lamina propria when the heat-inactivated *E. coli* were injected into the SHXB- and STC3-infected piglets 48 h later. Data express the mean ± SEM ($n = 5$). Bars labelled with different letters are significantly different from each other ($P < 0.05$).

functions to some extent. Next, the model antigen (the heat-inactivated *E. coli*) was used to further determine whether SHXB and STC3 could influence the functions of intestinal DCs. The results showed that after 15 min of injecting heat-inactivated *E. coli*, the $CD11b^+CD16^+$ DCs and $SWC3a^+SLA\text{-}II\text{-}DR^+$ DCs rapidly increased in the small intestine villi of only the injected heat-inactivated *E. coli* piglets, followed by the STC3-infected piglets, and were lowest in the SHXB-infected piglets (Fig. 6A and B). Then, these DCs in the intestinal villi of all groups gradually decreased and in the lamina propria gradually increased after 3 h. The number of these DCs in the intestinal villi and lamina propria in STC3-infected piglets was still highest among all groups 3 h after injecting heat-inactivated *E. coli* (Fig. 6A and B). At 3 h after injecting the heat-inactivated *E. coli*, the number of these DCs in villi of piglets infected with SHXB was equal to the control group, but the $CD11b^+CD16^+$ DCs in lamina propria of the piglets infected with SHXB were significant lower than others (Fig. 6A and B). These results indicated that STC3-infected piglets could enhance the ability of intestinal DCs to uptake the heat-inactivated *E. coli* and migrate to the lamina propria, whereas this ability was impaired in SHXB-infected piglets. The $CD3^+$, $CD4^+$, $CD8^+$ T cells were mainly distributed in the intestinal lamina propria of piglets. (see the Supplementary data (additional files 4)). These T cells rapidly increased in the small intestine villi and lamina propria of only injected heat-inactivated *E. coli* piglets and STC3-infected piglets from 15 min to 3 h after injecting the heat-inactivated *E. coli*, while these T cells had no changes in small intestine villi and lamina propria of the piglets infected with SHXB at a similar timepoint (Fig. 6C–E). This showed that the STC3-infected piglets had an enhanced ability of intestinal DCs to stimulate T-cell subset proliferation, while the SHXB-infected piglets had an impaired ability of intestinal DCs to stimulate T-cell subset proliferation.

4. Discussion

A recent report showed that the intestinal DC network consisted of DCs derived from monocytes and pre-DCs (Bogunovic et al., 2009). Therefore, porcine Mo-DCs were used for researching the relationship between porcine DCs and TGEV *in vitro*. Phenotypically, porcine Mo-DCs are characterised as $CD1a^+SLA\text{-}DR\text{-}II^+(MHC\text{-}II^+)CD80/86^+$ and $SWC3a^+(CD172a^+)$ (Summerfield and McCullough, 2009). *In vivo*, co-expression of CD16, SLA-DR-II, CD11b (CD11R1) and SWC3a has previously been described (Haverson et al., 2000) as being characteristic for DCs in the porcine intestinal lamina propria. In our work, the $CD1a^+SLA\text{-}DR\text{-}II^+CD80/86^+SWC3a^+$ Mo-DCs and $SLA\text{-}DR\text{-}II^+/CD16^+/CD11b^+/SWC3a^+$-DCs were used for *in vitro* and *in vivo* analyses.

A similar infectivity of SARS coronavirus (SARS-CoV) in human immature and mature DCs was previously observed (Law et al., 2005). Similar to SARS-CoV, both SHXB and STC3 also infected immature and mature Mo-DCs, but the infectivity in immature Mo-DCs was higher than in mature Mo-DCs. This may be because the major receptor of TGEV (Aminopeptidase N) is mainly distributed in immature Mo-DCs, and the endocytosis of immature Mo-DCs was also significantly higher than mature Mo-DCs (these data were not shown). A previous study showed that the virulent TGEV robustly infected and rapidly destroyed the villous epithelial cells in the porcine small intestine to cause the rapid death of piglets, while the attenuated virus had a poor ability to infect and evoke the sickness of the piglets (Kim and Chae, 2002). Our work was consistent with this, and we speculated that virulent TGEV increased their replication in DCs for their dissemination.

Maturation of DCs is a critical process that results in presenting viral antigens to activate T cells and initiating an antiviral immune response (Zhou et al., 2007). The phenomenon has been reported in the classical swine fever virus (Carrasco et al., 2004) and the PRRS virus (Peng et al., 2009). It is known that DCs present antigen with CD1a or SLA-II-DR as the first signal and CD80/86 as the second co-stimulatory signal to activate T cells (Bertram et al., 2004). SHXB may act by inhibiting Mo-DC maturation, because it significantly down-regulated the expression of CD1a and SLA-DR-II on the immature and mature Mo-DCs. Why did SHXB cause a reduction in CD1a and SLA-DR-II on the mature Mo-DCs? It is possible that virus infection resulted in a loss of TLR-4, which is essential for LPS responsiveness (Poltorak et al., 1998). The surface markers of STC3-infected immature and mature Mo-DCs changed slightly (Fig. 2C), which implied that STC3 caused a weak injury on the Mo-DCs. Similarly, the expression of CD40, CD80, MHC I and MHC II did not significantly change in chicken Mo-DCs infected by low pathogenicity avian influenza (LPAI), while the markers notably decreased on Mo-DCs infected by high pathogenicity avian influenza (HPAI) (Vervelde et al., 2012). In addition, there was a negligible change in CD80/86 expression on immature and mature Mo-DCs infected by SHXB or STC3. This suggested that virulent TGEV inhibit Mo-DCs maturation through decreasing the antigen-presenting molecules, rather than the co-stimulatory molecules. Furthermore, the downregulation of surface markers on the Mo-DCs infected with SHXB was not caused by their apoptosis.

Cytokine response induced by virus-infected Mo-DCs is another critical process that results in presenting viral antigens to activate T cells. IL-12, believed to be the principal Th1-type cytokine, is necessary for cell-mediated immunity (CMI) (Barchet et al., 2006). IFN-γ plays an important role in inducing immunostimulatory and immunomodulatory effects (Chen et al., 2009). IL-10 is a predominant Th2-type cytokine that can downregulate IL-12 production and CMI (Yang et al., 2007). In this article, the promotion of IL-12 and IFN-γ secretion both in immature and mature Mo-DCs infected by SHXB and STC3 strains implied that Mo-DCs developed Th1 immune responses to TGEV infection, which was similar to the report that Rotavirus (RV)-infected DCs promote their capacity to induce the polarisation of allogenic naive T cells towards a Th1 response (Narvaez et al., 2005). However, the virulent SHXB only produced a slight of IL-12 and IFN-γ, as little as possible to make the Mo-DCs clear themselves, while STC3, as a vaccine strain, induced the secretion of considerable cytokines to improve the immature Mo-DCs' immune response. A recent report

showed that only when the amount of a virulent virus reached a threshold, called virulence threshold, its virulence reached the strongest (Lancaster and Pfeiffer, 2012). In this study, it might because the number of SHXB did not reach its virulence threshold in the mature Mo-DCs, like the attenuated STC3 strain, thus no difference in the expression of IL-12 and IFN-γ in SHXB- and STC3-infected mature Mo-DCs was found in our work. The STC3 and SHXB strains failed to stimulate IL-10 secretion on the immature and mature Mo-DCs. Because DCs are central to the development of the acquired T-cell response, pathogens have evolved mechanisms to reduce the capacity of infected DCs to prime the adaptive immune response. Virulent SHXB infection inhibits Mo-DC maturation and secreting cytokines, so that infected Mo-DCs are potentially less able to stimulate T-cell responses, like dengue virus (DV) (Dejnirattisai et al., 2008). However, attenuated STC3 was unlike SHXB because it induced the Mo-DCs to stimulate T-cell proliferation at a DC/T ratio of 1:1. For the phenomenon that there is a minor but significant difference between the SHXB and STC3 infected mature cells only at a ratio of 1:1. It might that STC3 did not inhibit the expression of CD1a in the mature Mo-DCs, while SHXB suppress this compared with the control immature Mo-DCs. Moreover, the level of secreting IL-12 in STC3 infected mature Mo-DCs (233.67 pg ml^{-1}) was higher than SHXB infected mature Mo-DCs (185.67 pg ml^{-1}), thus it was possible that the significant difference between the SHXB and STC3 infected mature cells stimulated the T cells proliferation. From the results, we observed that the more it was in the number of Mo-DCs, the stronger it had the ability to activate the T cells proliferation. Thus there is a minor but significant difference between the SHXB and STC3 infected mature cells only at a DC/T ratio of 1:1 but not at the other ratios.

In order to further verify that SHXB strain severely impaired the functions of DCs *in vitro*, we carried out *in vivo* analyses. When encountering a virus, the DCs rapidly uptake the invading virus and migrate to the lymph nodes in order to activate T cells. Because of stronger virulence, SHXB robustly induced the intestinal epithelial cells to secrete the pro-inflammatory chemokines CCL20, CCL25 and CCL27, leading to a rapid recruitment of DCs and T cells to the intestinal villi (the data was not shown). Therefore, after 15 min of injection of SHXB, the number of $CD11b^+CD16^+$ DCs, $SWC3a^+SLA\text{-}DR\text{-}II^+$ DCs and $CD3^+$, $CD4^+$ and $CD8^+$ T cells in intestinal villi rapidly increased; such a response did not occur after STC3 injection. Having acquired the antigens, these DCs could migrate from intestinal villi to the lymph node for activating T cells, therefore, after 3 h of SHXB infection, the DCs gradually reduced in number in the intestinal villi, and increased in the lamina propria. After 48 h of virus infection, the number of DCs and $CD3^+$, $CD4^+$ and $CD8^+$ T cells in the intestinal villi and lamina propria of piglets infected with SHXB was significantly reduced; in contrast, there were significantly more of these cell types in STC3-infected piglets. These results suggest that SHXB significantly impaired the ability of porcine DCs to process and present antigens to activate T cells, and was consistent with that SHXB significantly damaged the ability of porcine Mo-DCs to process and present antigens to activate T cells *in vitro*. The STC3 strain was similar to the vaccine strain in that it enhanced the porcine DCs' ability to process and present antigens to stimulate $CD3^+$, $CD4^+$ and $CD8^+$ T-cell proliferation at 48 h postinfection. It is known that the CD3 protein complex is an important T cell marker for the maturation of T cells (Chetty and Gatter, 1994). $CD4^+$T cells play a central role in helping B cells make antibodies and inducing macrophages to develop enhanced microbicidal activity (Zhu and Paul, 2008). $CD8^+$ T-cells can kill virally infected target cells by secreting perforin and granzymes (Mosmann et al., 1997; Stenger et al., 1997). From our results, $CD4^+$ T cells accounted for 80–90% of the total $CD3^+$ T cells, while $CD8^+$ T cells were only 10–20% of the total $CD3^+$ T cells. Therefore, there was a tendency to develop humoral immunity for the intestinal mucosal immune response, and it also indirectly explained the important antiviral role of SIgA in mucosal immunity. Lastly, the model antigen (the heat-inactivated *E. coli*) was used to further prove that virulent and attenuated TGEV could influence the functions of intestinal DCs. The $CD11b^+CD16^+$ DCs and $SWC3a^+SLA\text{-}II\text{-}DR^+$ DCs in the piglets infected with STC3 had a higher ability to take up and migrate and stimulate T-cell proliferation. Nevertheless, these two intestinal DCs had a significantly damaged ability to take up, migrate and stimulate T-cell subset proliferation in the piglets infected with SHXB.

5. Conclusion

This study indicated that the SHXB strain severely impaired the ability of DCs to uptake, migrate, and induce the activation of T lymphocytes, while the STC3 strain enhanced these functions of DCs *in vitro* and *in vivo*. This might be due to the differences in pathogenesis of virulent and attenuated TGEV in piglets, and could help us to develop a better strategy to prevent TGEV infection by improving the functions of DCs. Furthermore, this study also provides a reference for the mucosally transmitted infectious diseases (pneumonia, tuberculosis, measles, HIV/AIDS, avian flu, SARS, and multidrug-resistant bacteria).

Conflict of interest statement

The authors declare that they have no competing interests.

Acknowledgements

This work was supported by grant number 31172302 from the National Science Grant of China and the Priority Academic Program Development of Jiangsu Higher Education Institutions (PAPD).

Appendix A. Supplementary data

Supplementary data associated with this article can be found, in the online version, at http://dx.doi.org/10.1016/j.vetmic.2014.03.017.

References

Ardavin, C., 2003. Origin, precursors and differentiation of mouse dendritic cellsNature reviews. Nat. Rev. Immunol. 3, 582–590.

Baize, S., Kaplon, J., Faure, C., Pannetier, D., Georges-Courbot, M.C., Deubel, V., 2004. Lassa virus infection of human dendritic cells and macrophages is productive but fails to activate cells. J. Immunol. 172, 2861–2869.

Barchet, W., Price, J.D., Cella, M., Colonna, M., MacMillan, S.K., Cobb, J.P., Thompson, P.A., Murphy, K.M., Atkinson, J.P., Kemper, C., 2006. Complement-induced regulatory T cells suppress T-cell responses but allow for dendritic-cell maturation. Blood 107, 1497–1504.

Bertram, E.M., Dawicki, W., Watts, T.H., 2004. Role of T cell costimulation in anti-viral immunity. Semin. Immunol.16 185–196.

Bogunovic, M., Ginhoux, F., Helft, J., Shang, L., Hashimoto, D., Greter, M., Liu, K., Jakubzick, C., Ingersoll, M.A., Leboeuf, M., Stanley, E.R., Nussenzweig, M., Lira, S.A., Randolph, G.J., Merad, M., 2009. Origin of the lamina propria dendritic cell network. Immunity 31, 513–525.

Carrasco, C.P., Rigden, R.C., Schaffner, R., Gerber, H., Neuhaus, V., Inumaru, S., Takamatsu, H., Bertoni, G., McCullough, K.C., Summerfield, A., 2001. Porcine dendritic cells generated in vitro: morphological, phenotypic and functional properties. Immunology 104, 175–184.

Carrasco, C.P., Rigden, R.C., Vincent, I.E., Balmelli, C., Ceppi, M., Bauhofer, O., Tache, V., Hjertner, B., McNeilly, F., van Gennip, H.G., McCullough, K.C., Summerfield, A., 2004. Interaction of classical swine fever virus with dendritic cells. J. Gen. Virol. 85, 1633–1641.

Chen, Y., Khanna, S., Goodyear, C.S., Park, Y.B., Raz, E., Thiel, S., Gronwall, C., Vas, J., Boyle, D.L., Corr, M., Kono, D.H., Silverman, G.J., 2009. Regulation of dendritic cells and macrophages by an anti-apoptotic cell natural antibody that suppresses TLR responses and inhibits inflammatory arthritis. J. Immunol. 183, 1346–1359.

Chetty, R., Gatter, K., 1994. CD3: structure, function, and role of immunostaining in clinical practice. J. Pathol. 173, 303–307.

Dejnirattisai, W., Duangchinda, T., Lin, C.L., Vasanawathana, S., Jones, M., Jacobs, M., Malasit, P., Xu, X.N., Screaton, G., Mongkolsapaya, J., 2008. A complex interplay among virus, dendritic cells, T cells, and cytokines in dengue virus infections. J. Immunol. 181, 5865–5874.

Frederick, G., Bohl, E., Cross, R., 1976. Pathogenicity of an attenuated strain of transmissible gastroenteritis virus for newborn pigs. Am. J. Vet. Res. 37, 165.

Gutzeit, C., Raftery, M.J., Peiser, M., Tischer, K.B., Ulrich, M., Eberhardt, M., Stockfleth, E., Giese, T., Sauerbrei, A., Morita, C.T., Schonrich, G., 2010. Identification of an important immunological difference between virulent varicella-zoster virus and its avirulent vaccine: viral disruption of dendritic cell instruction. J. Immunol. 185, 488–497.

Haggett, P., Gunawardena, K., 1964. Determination of population thresholds for settlement functions by the Reed–Muench method. Prof. Geogr. 16, 6–9.

Haverson, K., Singha, S., Stokes, C.R., Bailey, M., 2000. Professional and non-professional antigen-presenting cells in the porcine small intestine. Immunology 101, 492–500.

He, K.w., Lin, J.H., Huan, H.H., Ni, Y.X., Qian, Y.Q., He, J.H., Hou, J.B., 2001. Studies on cell cultivation and pathogenicity of attenuated transmissible gastroenteritis virus STC3 [J]. Chin. J. Vet. Sci. Technol. 31, 8–9.

Kim, B., Chae, C., 2002. Experimental infection of piglets with transmissible gastroenteritis virus: a comparison of three strains (Korean, Purdue and Miller). J. Comp. Pathol. 126, 30–37.

Krempl, C., Herrler, G., 2001. Sialic acid binding activity of transmissible gastroenteritis coronavirus affects sedimentation behavior of virions and solubilized glycoproteins. J. Virol. 75, 844–849.

Lancaster, K.Z., Pfeiffer, J.K., 2012. Viral population dynamics and virulence thresholds. Curr. Opin. Microbiol. 15, 525–530.

Laude, H., Charley, B., Gelfi, J., 1984. Replication of transmissible gastroenteritis coronavirus (TGEV) in swine alveolar macrophages. J. Gen. Virol. 65 (Pt 2), 327–332.

Law, H.K., Cheung, C.Y., Ng, H.Y., Sia, S.F., Chan, Y.O., Luk, W., Nicholls, J.M., Peiris, J.S., Lau, Y.L., 2005. Chemokine up-regulation in SARS-coronavirus-infected, monocyte-derived human dendritic cells. Blood 106, 2366–2374.

Masters, P.S., 2006. The molecular biology of coronaviruses. Adv. Virus Res. 66, 193–292.

Mosmann, T.R., Li, L., Sad, S., 1997. Functions of CD8 T-cell subsets secreting different cytokine patterns. Semin. Immunol. 9, 87–92.

Narvaez, C.F., Angel, J., Franco, M.A., 2005. Interaction of rotavirus with human myeloid dendritic cells. J. Virol. 79, 14526–14535.

Nielsen, N.O., Sautter, J.H., 1968. Infection of ligated intestinal loops with hemolytic *Escherichia coli* in the pig. Can. Vet. J.[nl]La revue veterinaire canadienne 9, 90–97.

Pannetier, D., Reynard, S., Russier, M., Journeaux, A., Tordo, N., Deubel, V., Baize, S., 2011. Human dendritic cells infected with the nonpathogenic Mopeia virus induce stronger T-cell responses than those infected with Lassa virus. J. Virol. 85, 8293–8306.

Peng, Y.T., Chaung, H.C., Chang, H.L., Chang, H.C., Chung, W.B., 2009. Modulations of phenotype and cytokine expression of porcine bone marrow-derived dendritic cells by porcine reproductive and respiratory syndrome virus. Vet. Microbiol. 136, 359–365.

Poltorak, A., He, X., Smirnova, I., Liu, M.-Y., Van Huffel, C., Du, X., Birdwell, D., Alejos, E., Silva, M., Galanos, C., 1998. Defective LPS signaling in C3H/HeJ and C57BL/10ScCr mice: mutations in Tlr4 gene. Science 282, 2085–2088.

Rescigno, M., Urbano, M., Valzasina, B., Francolini, M., Rotta, G., Bonasio, R., Granucci, F., Kraehenbuhl, J.P., Ricciardi-Castagnoli, P., 2001. Dendritic cells express tight junction proteins and penetrate gut epithelial monolayers to sample bacteria. Nat. Immunol. 2, 361–367.

Stenger, S., Mazzaccaro, R.J., Uyemura, K., Cho, S., Barnes, P.F., Rosat, J.P., Sette, A., Brenner, M.B., Porcelli, S.A., Bloom, B.R., Modlin, R.L., 1997. Differential effects of cytolytic T cell subsets on intracellular infection. Science 276, 1684–1687.

Summerfield, A., McCullough, K.C., 2009. The porcine dendritic cell family. Dev. Comp. Immunol. 33, 299–309.

Vervelde, L., Reemers, S.S., van Haarlem, D.A., Post, J., Claassen, E., Rebel, J.M., Jansen, C.A., 2012. Chicken dendritic cells are susceptible to highly pathogenic avian influenza viruses which induce strong cytokine responses. Dev. Comp. Immunol. 39, 198–206.

Woods, R.D., 2001. Efficacy of a transmissible gastroenteritis coronavirus with an altered ORF-3 gene. Can. J. Vet. Res. 65, 28.

Yang, Z.F., Ho, D.W., Ngai, P., Lau, C.K., Zhao, Y., Poon, R.T., Fan, S.T., 2007. Antiinflammatory properties of IL-10 rescue small-for-size liver grafts. Liver Transpl. 13, 558–565 (official publication of the American Association for the Study of Liver Diseases and the International Liver Transplantation Society).

Zhou, W., Peng, Q., Li, K., Sacks, S.H., 2007. Role of dendritic cell synthesis of complement in the allospecific T cell response. Mol. Immunol. 44, 57–63.

Zhu, J., Paul, W.E., 2008. CD4 T cells: fates, functions, and faults. Blood 112, 1557–1569.